

SANDIA REPORT

SAND2006-3750

Unlimited Release

Printed June 2006

Finite Element Analyses of Continuous Filament Ties for Masonry Applications: Final Report for The Arquin Corporation

Clifford K. Ho, Tiffany A. Bibeau and Armando Quinones Sr.

Prepared by
Sandia National Laboratories
Albuquerque, New Mexico 87185 and Livermore, California 94550

Sandia is a multiprogram laboratory operated by Sandia Corporation,
a Lockheed Martin Company, for the United States Department of Energy's
National Nuclear Security Administration under Contract DE-AC04-94AL85000.

Approved for public release; further dissemination unlimited.



Issued by Sandia National Laboratories, operated for the United States Department of Energy by Sandia Corporation.

NOTICE: This report was prepared as an account of work sponsored by an agency of the United States Government. Neither the United States Government, nor any agency thereof, nor any of their employees, nor any of their contractors, subcontractors, or their employees, make any warranty, express or implied, or assume any legal liability or responsibility for the accuracy, completeness, or usefulness of any information, apparatus, product, or process disclosed, or represent that its use would not infringe privately owned rights. Reference herein to any specific commercial product, process, or service by trade name, trademark, manufacturer, or otherwise, does not necessarily constitute or imply its endorsement, recommendation, or favoring by the United States Government, any agency thereof, or any of their contractors or subcontractors. The views and opinions expressed herein do not necessarily state or reflect those of the United States Government, any agency thereof, or any of their contractors.

Printed in the United States of America. This report has been reproduced directly from the best available copy.

Available to DOE and DOE contractors from
U.S. Department of Energy
Office of Scientific and Technical Information
P.O. Box 62
Oak Ridge, TN 37831

Telephone: (865)576-8401
Facsimile: (865)576-5728
E-Mail: reports@adonis.osti.gov
Online ordering: <http://www.osti.gov/bridge>

Available to the public from
U.S. Department of Commerce
National Technical Information Service
5285 Port Royal Rd
Springfield, VA 22161

Telephone: (800)553-6847
Facsimile: (703)605-6900
E-Mail: orders@ntis.fedworld.gov
Online order: <http://www.ntis.gov/help/ordermethods.asp?loc=7-4-0#online>



SAND2006-3750
Unlimited Release
Printed June 2006

Finite Element Analyses of Continuous Filament Ties for Masonry Applications: Final Report for The Arquin Corporation

Clifford K. Ho and Tiffany A. Bibeau
Sandia National Laboratories
P.O. Box 5800
Albuquerque, New Mexico 87185
ckho@sandia.gov
(505) 844-2384

Armando Quinones, Sr.
Arquin Corporation
P.O. Box 876
La Luz, NM 88337
aava2003@yahoo.com
(505) 434-9590

Abstract

Finite-element analyses were performed to simulate the response of a hypothetical masonry shear wall with and without continuous filament ties to various lateral loads. The loads represented three different scenarios: (1) 100 mph wind, (2) explosive attack, and (3) an earthquake. In addition, a static loading analysis and cost comparison were performed to evaluate optimal materials and designs for the spacers affixed to the filaments. Results showed that polypropylene, ABS, and polyethylene (high density) were suitable materials for the spacers based on performance and cost, and the short T-spacer design was optimal based on its performance and functionality. Results of the shear-wall loading simulations revealed that simulated walls with the continuous filament ties yielded factors of safety that were at least ten times greater than those without the ties. In the explosive attack simulation (100 psi), the simulated wall without the ties failed (minimum factor of safety was less than one), but the simulated wall with the ties yielded a minimum factor of safety greater than one. Simulations of the walls subject to lateral loads caused by 100 mph winds (0.2 psi) and seismic events with a peak ground acceleration of 1 “g” (0.66 psi) yielded no failures with or without the ties. Simulations of wall displacement during the seismic scenarios showed that the wall with the ties resulted in a maximum displacement that was 20% less than the wall without the ties.

Acknowledgments

The authors would like to thank Jennifer Lee Sinsabaugh of the Small Business Assistance Program for supporting the collaboration between Sandia National Laboratories and the Arquin Corporation and for providing administrative assistance during this project. The work described in this report was funded through the New Mexico Small Business Assistance initiative at Sandia National Laboratories. Neither Sandia nor the U.S. Government acquired any rights in any Arquin Corporation intellectual property as a result of this work.

Sandia is a multiprogram laboratory operated by Sandia Corporation, a Lockheed Martin Company for the United States Department of Energy's National Nuclear Security Administration under contract DE-AC04-94AL85000.

Contents

1. Introduction.....	9
2. Evaluation of Plastic Materials and Designs	10
2.1 Analysis of Static Loading Caused by 12-Foot Wall.....	10
2.2 Cost Analysis of Different Plastic Materials	15
2.3 Material and Design Recommendations.....	16
3. Lateral Loading of Walls With and Without Continuous Filament Ties.....	16
3.1 Model Approach.....	17
3.1.1 Boundary Conditions	18
3.2 Results and Discussion.....	19
4. Summary.....	25
5. References.....	25

List of Figures

Figure 1. Left: Prototype designs made of wood for the Arquin spacer. Right: Filaments (ties) comprised of the spacers and 9-gage steel wires are laid on top of a CMU.....	9
Figure 2. Left: Filaments of ties provide spacing and alignment for rows of CMUs. Right: Assembly of CMUs and filaments.....	10
Figure 3. SolidWorks® models of the short T-spacer (top left), long T-spacer (top right), and bowtie spacer (bottom). All dimensions are in inches.	11
Figure 4. Loading conditions for the short T-spacer (top left), long T-spacer (top right), and bowtie spacer (bottom). Green arrows denote constraints; purple arrows denote loads.	12
Figure 5. Representative images from the short T-spacer simulations. Top left: ABS displacement plot. Top right: PVC displacement plot. Bottom left: ABS factor of safety plot. Bottom right: PVC factor of safety plot.....	13
Figure 6. Representative images from the long T-spacer simulations. Top left: polyethylene displacement plot. Top right: PVC displacement plot. Bottom left: polyethylene factor of safety plot. Bottom right: PVC factor of safety plot.	14
Figure 7. Representative images from the bowtie-spacer simulations. Top left: polypropylene displacement plot. Top right: PVC displacement plot. Bottom left: polypropylene factor of safety plot. Bottom right: PVC factor of safety plot.	15
Figure 8. Force generated on a shear wall as a result of ground acceleration from an earthquake.....	17
Figure 9. Top left: Single steel-wire filament with short T-spacers. Top right: Assembled row with CMU blocks and two filaments (underside view). Bottom left: Mortar cavity for CMU wall with spacers. Bottom right: Assembled wall with filaments and mortar, ready for analysis.....	18
Figure 10. Boundary conditions applied to the simulated CMU wall. Left: 100 mph wind and explosive attack. Right: Seismic event. Green arrows denote restraints. Red arrows denote lateral pressure (loads).	19
Figure 11. Results of lateral loading on a wall without ties for 100 mph wind (top) and explosive blast (bottom). Displacement plots are on the left, and factor of safety plots are on the right (the FOS plot shows only two colors: blue if FOS > 1 and red if FOS < 1).	21
Figure 12. Results of lateral loading on a wall with ties (dual filaments with polypropylene short T-spacers) for 100 mph wind (top) and explosive blast (bottom).	

Displacement plots are on the left, and factor of safety plots are on the right (the FOS plot shows only two colors: blue if $FOS > 1$ and red if $FOS < 1$)......22

Figure 13. Top left: Maximum stress plot of the CMU wall with ties. Top right: Close-up image of the max stress on a section view of the CMU wall with ties. Bottom: Section view of the CMU wall that shows the steel filament in the mortar between the CMU blocks that absorbed the stress.....23

Figure 14. Simulated resultant displacement (left) and stress distribution (right) of CMU wall without ties for seismic event.....24

Figure 15. Simulated resultant displacement (left) and stress distribution (right) of CMU wall with ties for seismic event.....24

Figure 16. Cut-planes showing location of maximum simulated stress in the CMU wall with ties for the seismic scenario. In the expanded view on the right, the highest stresses are shown to occur along the steel filament under the polypropylene spacer (blue outline).....25

List of Tables

Table 1. Summary of material properties used in the finite-element analyses.	10
Table 2. Static loading results for the different plastic materials and spacer designs.	12
Table 3. Cost comparison of plastics and spacer designs.	16
Table 4. Simulation comparisons between the CMU wall with and without continuous filament ties.	20

1. Introduction

The Arquin Corporation, a New Mexico company, is developing continuous filament ties that are intended to increase the fabricating efficiency and strength of masonry shear walls comprised of concrete modular units (CMU) and other materials such as bricks. The ties are composed of spacers affixed to 9-gage steel wire that are laid on top of each row of the wall (Figure 1). The spacers provide accurate spacing and alignment for each CMU or brick that is laid on top, and the assembled ties are also intended to provide additional structural integrity when laid in between each row of the wall (Figure 2).

Arquin contacted Sandia National Laboratories' Small Business Assistance Program to obtain technical assistance in the following areas:

1. *Identification of suitable plastic materials and designs for spacers for optimal performance and lowest cost.* The material should not yield upon static loading under the weight of the wall, and the material should be amenable to injection molding processes.
2. *Evaluation of enhanced structural integrity of walls with ties.* Simulations should be performed to determine if the ties provide additional strength and deformation resistance to lateral loads caused by high winds, nearby explosions, or seismic events.

The remainder of this report presents simulations, analyses, and discussions regarding each of these areas.

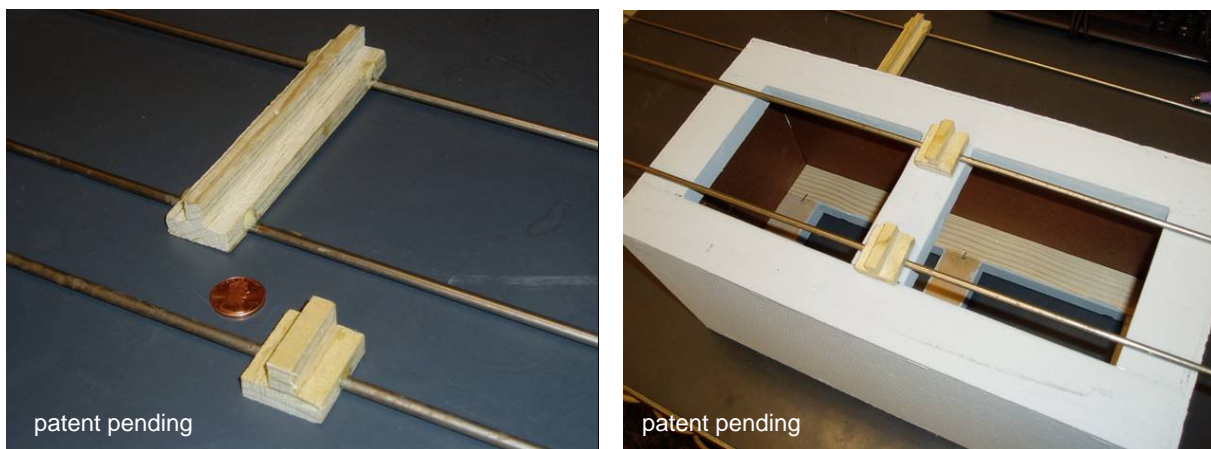


Figure 1. Left: Prototype designs made of wood for the Arquin spacer. Right: Filaments (ties) comprised of the spacers and 9-gage steel wires are laid on top of a CMU.

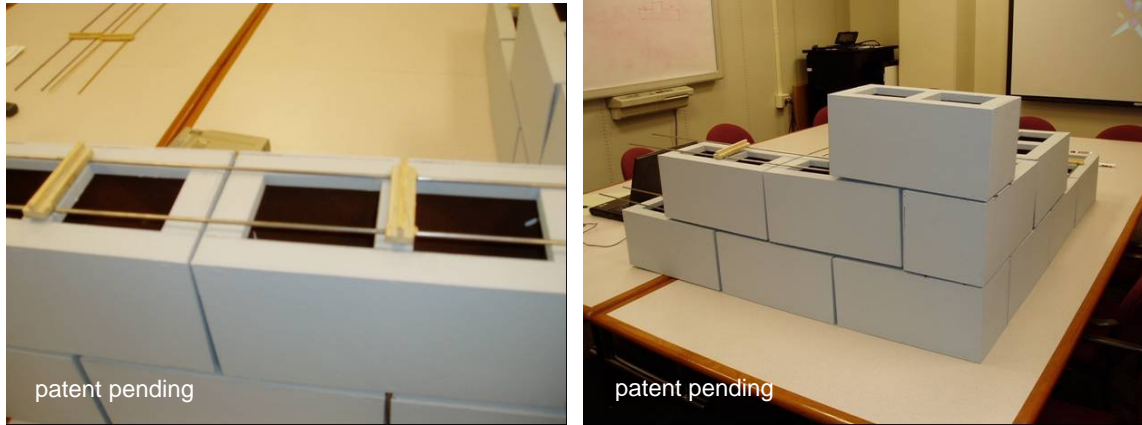


Figure 2. Left: Filaments of ties provide spacing and alignment for rows of CMUs. Right: Assembly of CMUs and filaments.

2. Evaluation of Plastic Materials and Designs

2.1 Analysis of Static Loading Caused by 12-Foot Wall

An analysis was performed to simulate static loading on the spacers caused by a 12-foot high wall. Three different spacer designs were evaluated: (1) short T-spacer, (2) long T-spacer, and (3) bowtie spacer. SolidWorks[®] was used to create three-dimensional models of the different designs (Figure 3). In addition, six different plastic materials were evaluated for each design: polypropylene (PP), acrylonitrile butadiene styrene (ABS), acrylic, polyvinyl chloride (PVC-plasticized), polyethylene (PE-high density), and polytetrafluoroethylene (PTFE or teflon). The material properties used in the analyses are summarized in Table 1.

Table 1. Summary of material properties used in the finite-element analyses.

	Density (kg/m ³):	Modulus of Elasticity (GPa):	Poisson's Ratio:	Yield Strength (MPa):
Concrete ^a	2480	30.0	0.20	37.3*
Mortar ^b	2240	11.17	0.15	12.4*
Polypropylene ^c	905	0.896	0.4103	23.8
ABS ^c	1020	2.0	0.3940	30.0
Acrylic ^c	1200	2.4	0.350	206.8
PVC-Plasticized ^c	1290	0.006	0.47	13.0
PE-High Density ^c	952	1.07	0.4101	22.1
PTFE ^c	2170	0.40	0.46	20.7
Steel Alloy ^c	7700	211	.28	620.42

*The strength of concrete and mortar is measured in compression.

^a Callister (2003)

^b Material properties identified by: *Portland Cement Assoc.* www.cement.org phone: 847.966.6200

^c Material properties identified in *SolidWorks*[®] 2004 Materials Database (www.solidworks.com).

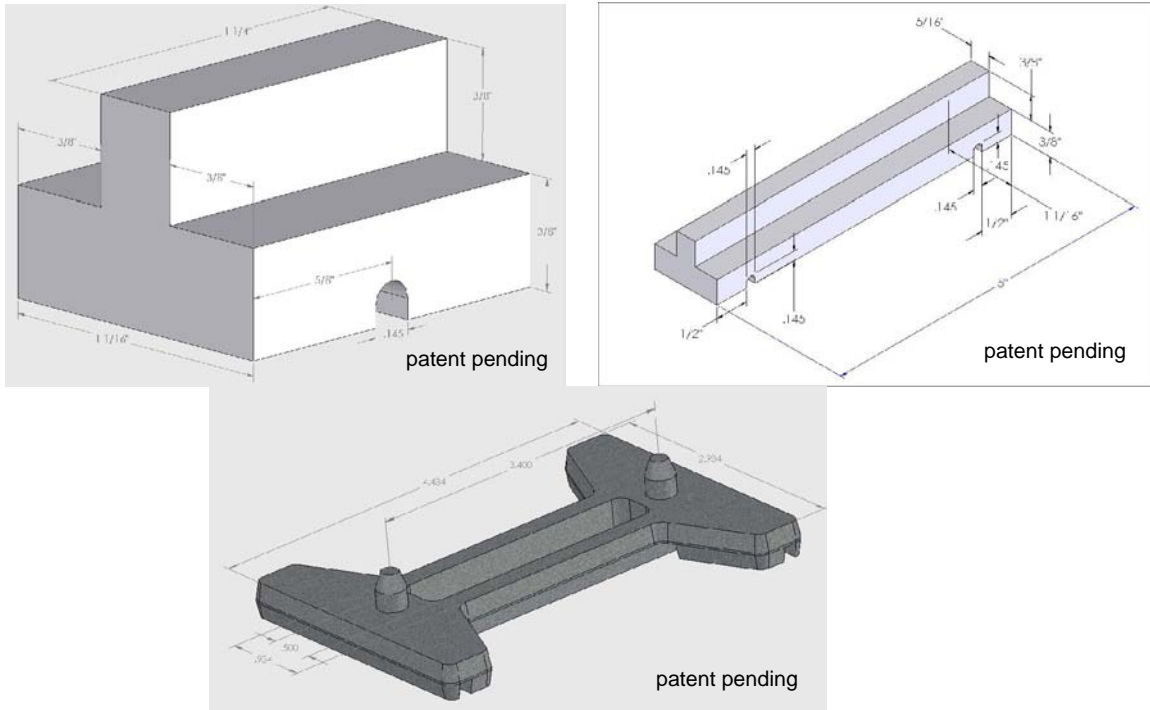


Figure 3. SolidWorks® models of the short T-spacer (top left), long T-spacer (top right), and bowtie spacer (bottom). All dimensions are in inches.

A total loading of 900 lbs was applied to the top surface of each spacer design to simulate the weight of a 12-foot high wall.¹ The load on each surface of the spacer is calculated by dividing the total load by the number of supporting surfaces. For example, each shoulder of the short T-spacer is loaded with 225 lbs. ($900 \div 4$) since the weight of each CMU is supported by a total of four “shoulder” surfaces. The loading on each shoulder of the long T-spacer is 450 lbs since the weight of each CMU is supported by only two shoulder surfaces with the long T-spacer configuration. Finally, the surface of the bowtie spacer is continuous (no shoulders) and supports the entire 900 lbs. The different loadings and the finite-element mesh are shown in Figure 4 for each design. The bottom of each spacer was completely constrained.

CosmosWorks™ was used to perform a finite-element stress analysis using the boundary conditions identified in Figure 4. Table 2 summarizes the maximum stress, maximum displacement, and minimum factor of safety (FOS) simulated for each of the different materials and spacer designs.

¹ Each CMU weighs approximately 50 pounds, and there are 18 rows in a 12-foot-high wall. Since a spacer is placed on the centerline of each CMU, the weight sustained by the bottom spacer(s) is equal to $18 \times 50 = 900$ pounds.

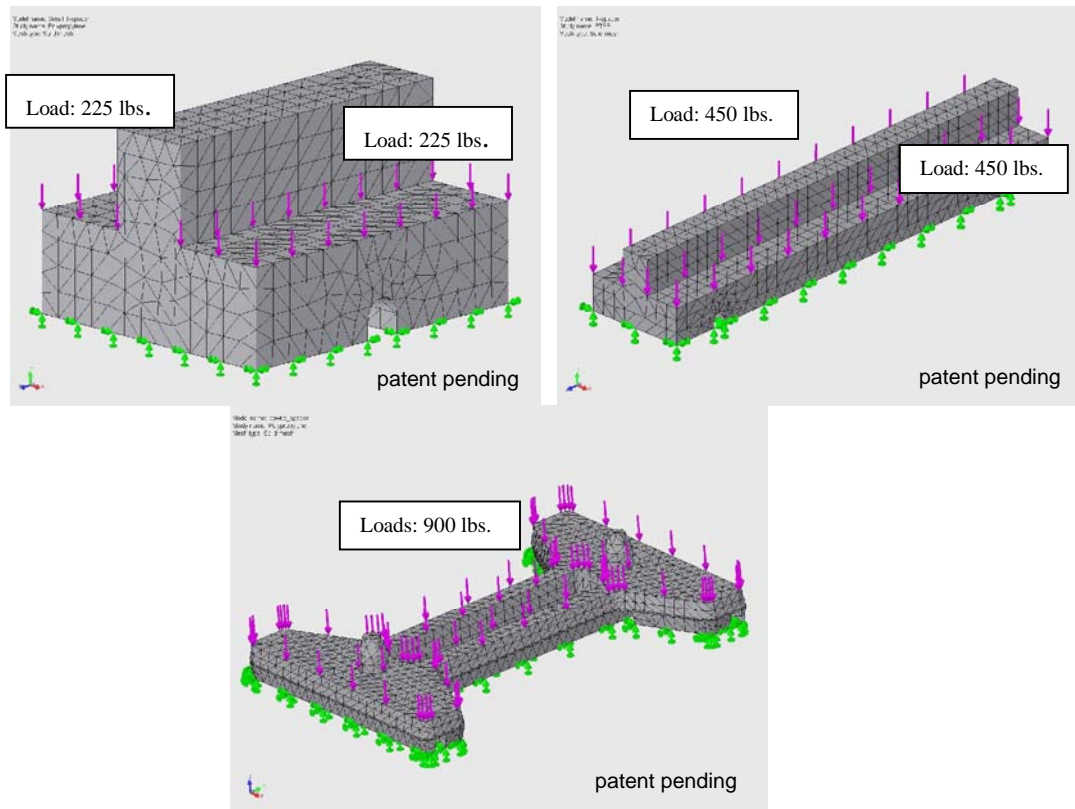


Figure 4. Loading conditions for the short T-spacer (top left), long T-spacer (top right), and bowtie spacer (bottom). Green arrows denote constraints; purple arrows denote loads.

Table 2. Static loading results for the different plastic materials and spacer designs.

Design	Result	Material					
		PP	ABS	Acrylic	PVC	PE	PTFE
Short T-spacer	Max. Stress (MPa)	7.128	7.086	7.103	7.345	7.127	7.789
	Max. Displacement (mm)	0.0467	0.0209	0.0175	7.129	0.0391	0.1063
	FOS	3.3	4.2	29	1.8	3.1	2.8
Long T-spacer	Max. Stress (MPa)	3.755	3.744	3.722	3.813	3.755	3.8
	Max. Displacement (mm)	0.0238	0.0105	0.0024	3.725	0.0199	0.0482
	FOS	6.3	8	56	3.4	5.9	5.4
Bowtie Spacer	Max. Stress (MPa)	3.834	3.856	4.188	3.787	3.835	3.715
	Max. Displacement (mm)	0.0207	0.0940	0.0813	2.916	0.0173	0.0439
	FOS	6.2	6.2	49	3.4	5.8	5.6

FOS = factor of safety (yield strength of material divided by maximum applied stress)

The results show that all of the plastic materials except for PVC produce acceptable results with regard to maximum displacement (deformation) and factor of safety. The maximum displacement simulated for PVC is 7 mm for the short T-spacer design and 3-4 mm for the other designs. The simulated factor of safety is at least three for nearly all three designs except for the short T-spacer design using PVC, which yields a factor of safety of 1.8. Figure 5 through Figure 7 show representative images from the static-load simulations. In each figure, a material with acceptable results is shown on the left, and a material with unacceptable results is shown on the right. The images show plots of the displacement distribution and the factor-of-safety distribution on each design for the representative materials.

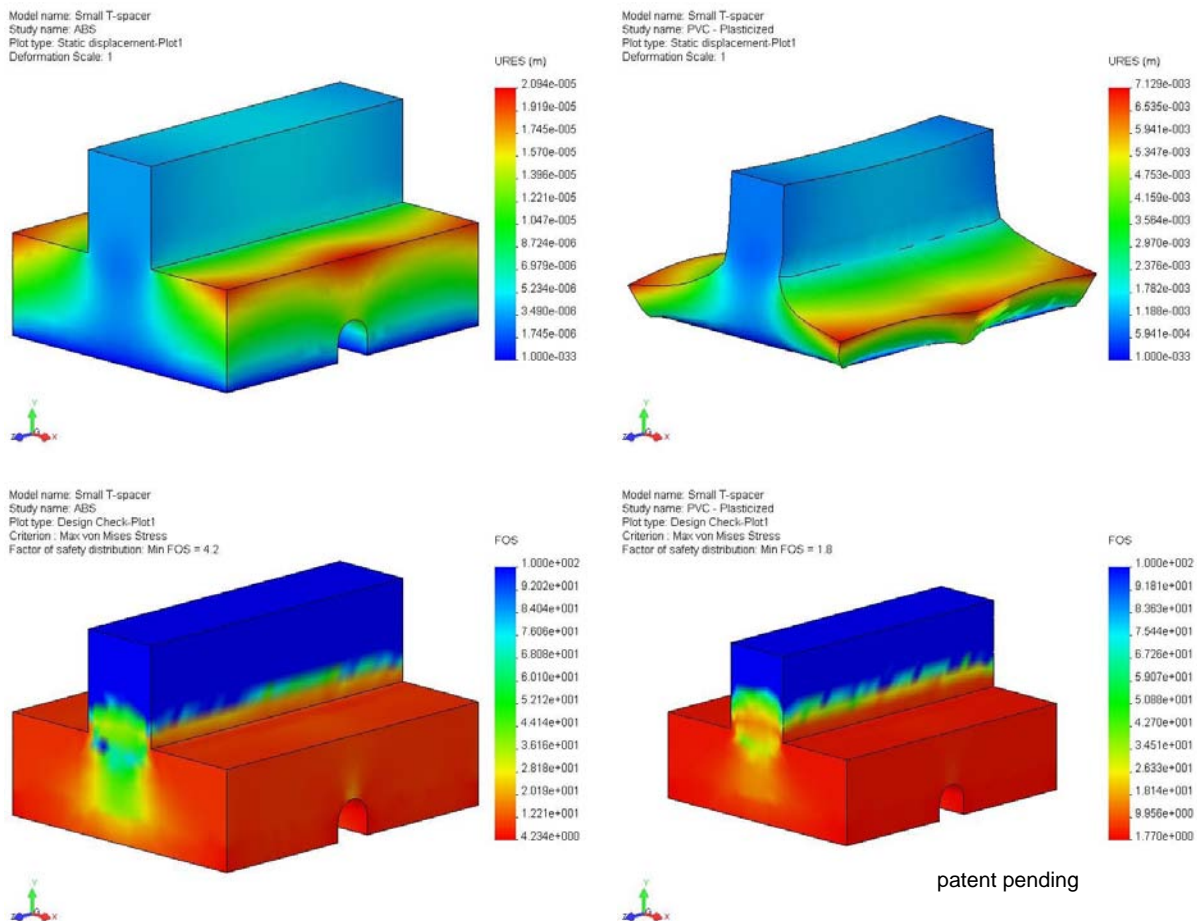
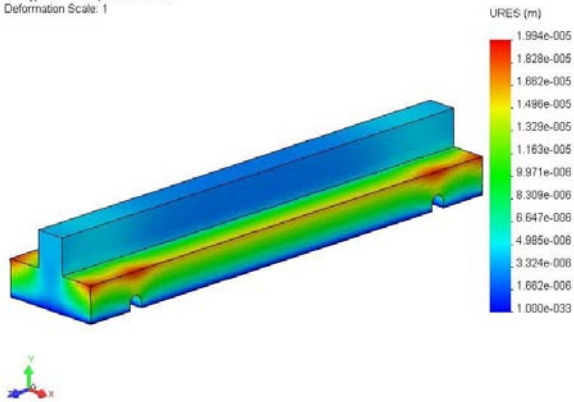
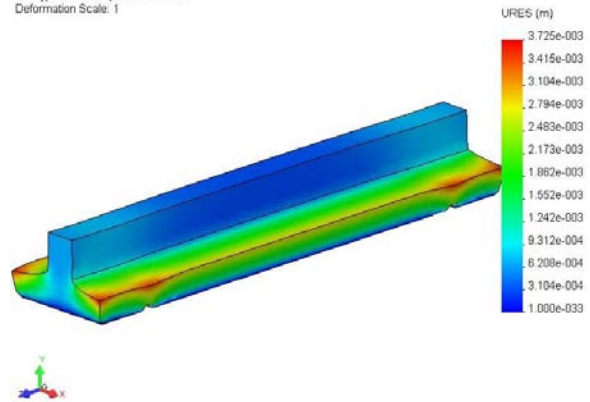


Figure 5. Representative images from the short T-spacer simulations. Top left: ABS displacement plot. Top right: PVC displacement plot. Bottom left: ABS factor of safety plot. Bottom right: PVC factor of safety plot.

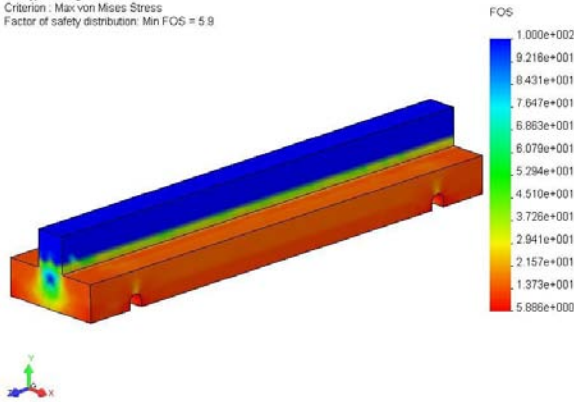
Model name: T-spacer
Study name: PE
Plot type: Static displacement-Plot1
Deformation Scale: 1



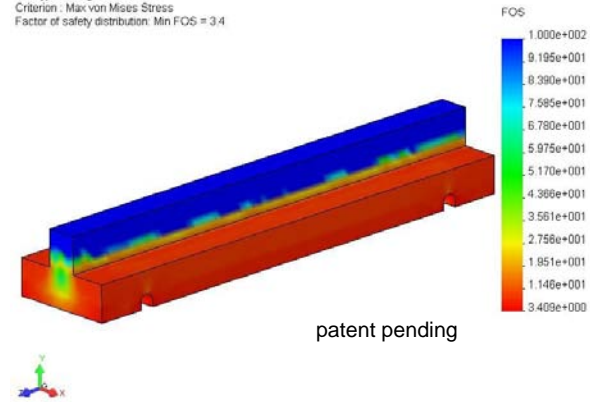
Model name: T-spacer
Study name: PVC
Plot type: Static displacement-Plot1
Deformation Scale: 1



Model name: T-spacer
Study name: PE
Plot type: Design Check-Plot1
Criterion: Max von Mises Stress
Factor of safety distribution: Min FOS = 5.9



Model name: T-spacer
Study name: PVC
Plot type: Design Check-Plot1
Criterion: Max von Mises Stress
Factor of safety distribution: Min FOS = 3.4



patent pending

Figure 6. Representative images from the long T-spacer simulations. Top left: polyethylene displacement plot. Top right: PVC displacement plot. Bottom left: polyethylene factor of safety plot. Bottom right: PVC factor of safety plot.

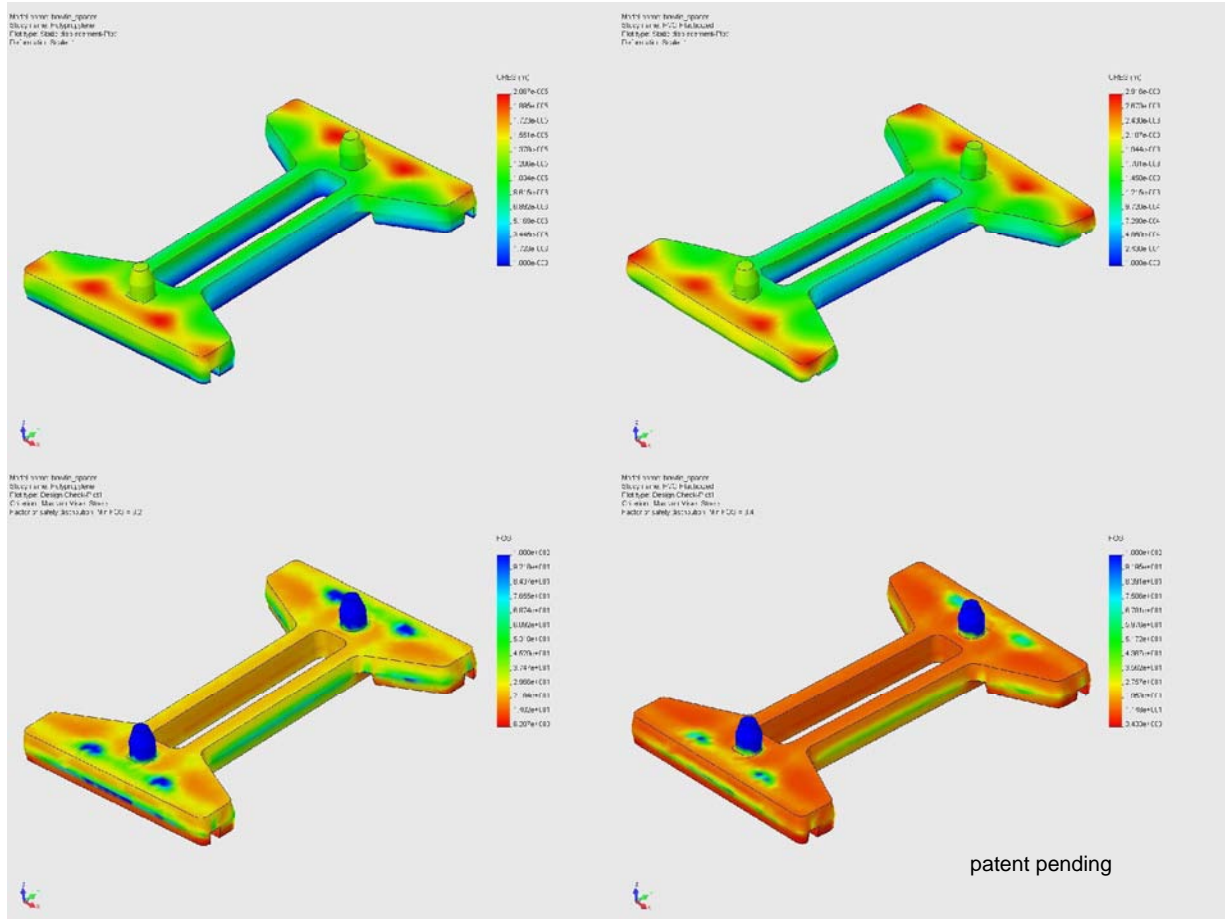


Figure 7. Representative images from the bowtie-spacer simulations. Top left: polypropylene displacement plot. Top right: PVC displacement plot. Bottom left: polypropylene factor of safety plot. Bottom right: PVC factor of safety plot.

2.2 Cost Analysis of Different Plastic Materials

In addition to performance (deformation and factor of safety), cost is another issue that was evaluated among the different materials and designs. Table 3 shows a cost comparison among the materials and designs based on the simulated volume and mass of each part and the reported cost per pound of the different plastics. Polypropylene is the cheapest material, followed by polyethylene, PVC, ABS, acrylic, and then PTFE. Among the different designs, the short T-spacer is the cheapest, followed by the bowtie design and the long T-spacer. The resulting unit cost is for the raw material only, and this price can vary depending on the vendor and the amount of plastic purchased.

Table 3. Cost comparison of plastics and spacer designs.

Design	Feature	Materials Amenable to Injection Molding					
		PP	ABS	Acrylic	PVC	PE	PTFE
Short T-spacer	Volume (cm ³)	10.24	10.24	10.24	10.24	10.24	10.24
	Mass (lbs)	0.02	0.023	0.027	0.029	0.021	0.052
	Cost (per pound)*	\$3.20	\$4.12	\$5.32	\$3.90	\$3.40	\$99.40
	Cost (per unit)	\$0.064	\$0.095	\$0.144	\$0.113	\$0.071	\$5.17
Long T-spacer	Volume (cm ³)	41.59	41.59	41.59	41.59	41.59	41.59
	Mass (lbs)	0.083	0.094	0.110	0.118	0.087	0.213
	Cost (per pound)*	\$3.20	\$4.12	\$5.32	\$3.90	\$3.40	\$99.40
	Cost (per unit)	\$0.266	\$0.387	\$0.585	\$0.460	\$0.296	\$21.17
Bowtie Spacer	Volume (cm ³)	32.20	32.20	32.20	32.20	32.20	32.20
	Mass (lbs)	0.064	0.072	0.085	0.092	0.068	0.165
	Cost (per pound)*	\$3.20	\$4.12	\$5.32	\$3.90	\$3.40	\$99.40
	Cost (per unit)	\$0.205	\$0.297	\$0.452	\$0.359	\$0.231	\$16.40

*Cost per pound of raw material when purchased in small quantities (price will reduce with large quantity orders). KEYTEC, INC. Richardson, TX www.magictouch.com phone: 972.234.8617

2.3 Material and Design Recommendations

Based on the results of the static-loading simulations and the cost comparisons, we recommend the following materials: polypropylene, ABS, and polyethylene (high density). These materials performed well with regard to the simulated performance metrics of displacement and factor of safety, and they were the least expensive. These materials are also amenable to injection molding processes.

With regard to the design, we recommend the short T-spacer design because of its acceptable performance, lowest cost, and the following functionality:

- The single-filament short T-spacer design allows a variable width between two filaments
- More than two filaments can be used depending on pilaster width (e.g., three filaments can be used for wide pilasters)
- Packaging and shipment will be easier with the short T-spacer
- The short T-spacers can be used for single-filament applications (e.g., veneer wall with 2"x4"x8" bricks)

3. Lateral Loading of Walls With and Without Continuous Filament Ties

Simulations were performed to determine if the continuous filament masonry ties provided additional integrity and safety to CMU shear walls. Lateral loads were applied to the side of a

CMU shear wall to simulate three different scenarios: (1) 100 mph winds, (2) a nearby explosion, and (3) an earthquake. Masonry walls are typically designed to withstand wind loads up to 100 mph (International Building Code, 2003), which, according to theoretical and empirical drag correlations, corresponds to approximately 0.2 psi of pressure against a flat two-dimensional wall (Roberson and Crowe, 1985). However, an explosive blast can produce significantly higher peak pressures on the order of 100 psi on a nearby wall or building.²

In addition, ground motion from earthquakes can impose an inertial force on shear walls that is equivalent to a lateral load (Figure 8). Although many different loading scenarios could be imparted from different types of seismic motions (e.g., P-wave, S-wave, Love Wave, Rayleigh Wave) and spectral energy distributions, the approach taken in this study was to choose a conservative estimate of the peak ground acceleration that could be used to calculate an effective lateral load on the shear wall. The United States Geological Survey publishes probabilistic seismic hazard assessment maps that give the annual probability of experiencing a particular ground acceleration from earthquakes in various regions. Petersen et al. (1996) report that a peak ground acceleration of 1 “g” (9.81 m/s²) can be expected to occur in southern California approximately once every thousand years. According to studies by Wald et al. (1999) and Trifunac and Brady (1975), a peak ground acceleration of 9.81 m/s² corresponds to a Modified Mercalli Intensity between IX and X, which is comparable to a >7.0 magnitude earthquake on the Richter scale.³ This value for the peak ground acceleration was used as a conservative estimate to calculate the applied load that could be experienced by shear walls during earthquakes.

Simulations of walls subject to these conditions and scenarios were performed with and without the continuous filament ties, and the results were compared.

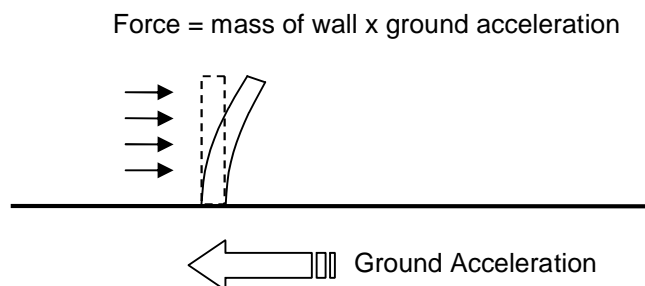


Figure 8. Force generated on a shear wall as a result of ground acceleration from an earthquake.

3.1 Model Approach

A 4' x 8' wall was constructed in SolidWorks[®] with and without the continuous filament ties. For the model with the ties, the CMU blocks were stacked together and mated to mortar, which filled all the cavities. For the model with ties, each filament was simulated, and then a row of

² <http://www.globalsecurity.org/military/systems/munitions/damage.htm>

³ http://earthquake.usgs.gov/learning/topics/mag_vs_int.php

CMU blocks was simulated on top of each pair of filaments. The rows were stacked and mortar was used to fill the cavities (see Figure 9). The total number of elements used in the finite-element simulations for the wall with and without ties was 363,189 elements and 265,059 elements, respectively. The spacer material and design used for the simulations was the polypropylene short T-spacer (two single filaments per row). It was chosen due to its good performance under a static load and low production cost. Table 1 lists the material properties for the polypropylene, concrete, mortar, and steel filaments that were used in the analysis.

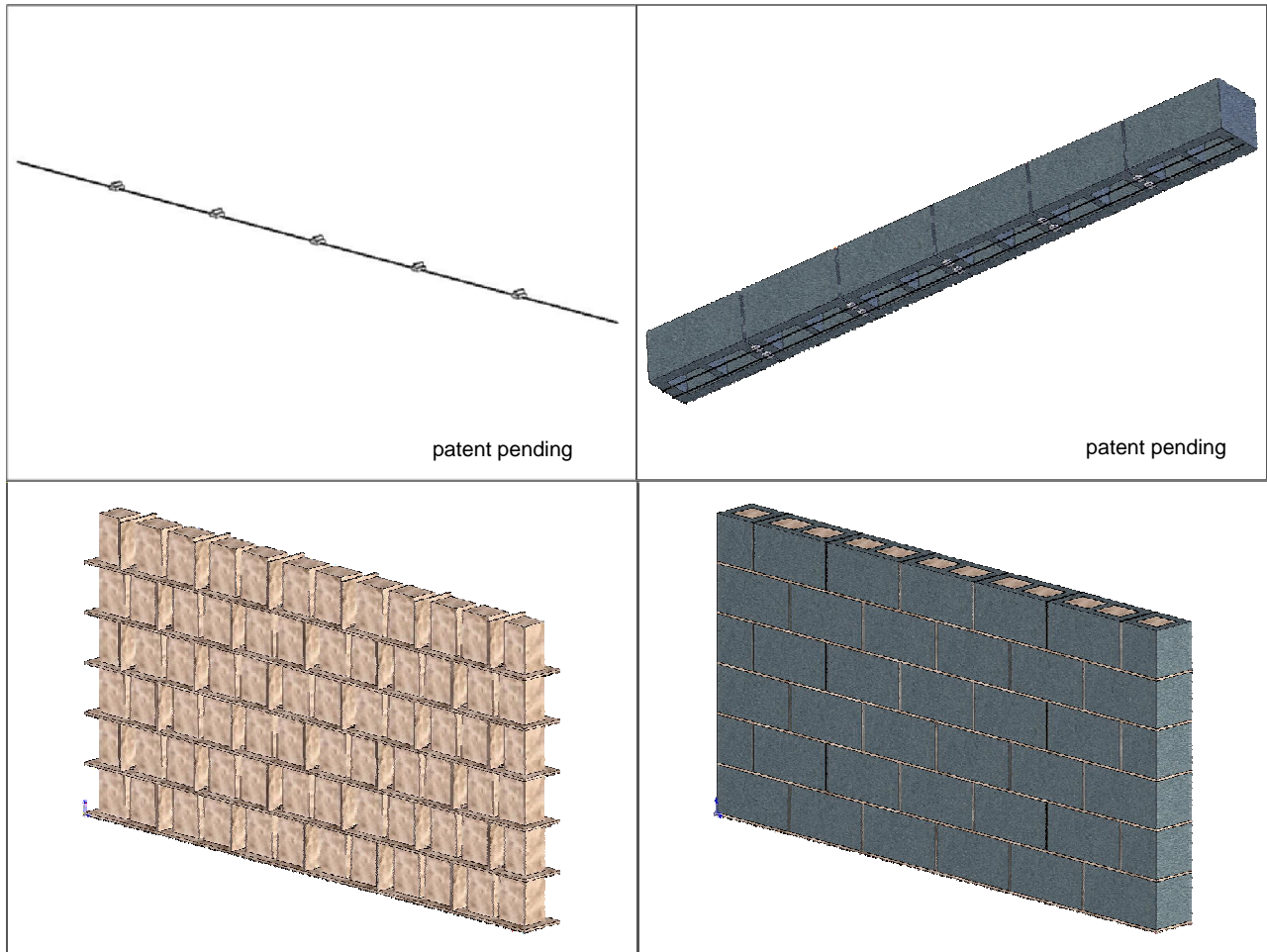


Figure 9. Top left: Single steel-wire filament with short T-spacers. Top right: Assembled row with CMU blocks and two filaments (underside view). Bottom left: Mortar cavity for CMU wall with spacers. Bottom right: Assembled wall with filaments and mortar, ready for analysis.

3.1.1 Boundary Conditions

Different boundary conditions were applied to the simulated wall in each of the three loading scenarios. For the 100 mph wind and explosive attack, the wall was restrained on the bottom and sides. For the seismic event, the wall was restrained only along the bottom. The difference was due to the assumption that the wind and explosive attack originated from *outside* the wall, and

additional perpendicular interior walls provided additional support and restraint along the sides of the wall. In the seismic scenario, it was assumed that the oscillating motion of the ground could cause the shear wall to move *away* from any interior walls; therefore, only bottom restraints were simulated. A lateral load of 0.2 psi was applied to the face of the shear wall to represent the high wind, and a lateral load of 100 psi was applied to the front faces of the CMU blocks and mortar to represent an explosive blast. For the seismic scenario, a peak ground acceleration of 9.81 m/s^2 was multiplied by the mass of the wall (1,356 kg) to yield an effective lateral load of 13,300 N ($\sim 3,000 \text{ lb}_f$). Distributed over the area of the wall (3 m^2 or 32 ft^2), the effective pressure applied to the wall was 4580 Pa or 0.66 psi. See Figure 10 for a schematic of the applied boundary conditions for the different scenarios.

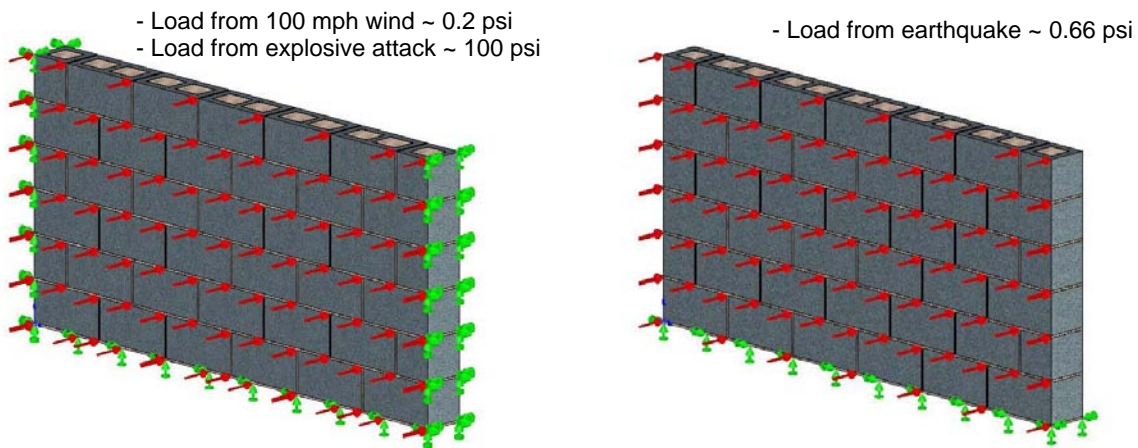


Figure 10. Boundary conditions applied to the simulated CMU wall. Left: 100 mph wind and explosive attack. Right: Seismic event. Green arrows denote restraints. Red arrows denote lateral pressure (loads).

3.2 Results and Discussion

A summary of the simulation results is presented in Table 4. The results show that the simulated wall performs well with or without ties when subjected to a 100 mph wind (0.2 psi). The simulated maximum displacement is just over 6 microns, and the factor of safety (FOS) is well above 100 in both cases. However, the simulated explosive blast causes the simulated wall without ties to fail (i.e., the factor of safety drops below one), and the simulated displacement is on the order of several millimeters. In contrast, the simulated explosive blast against the wall with ties does not fail; its minimum factor of safety is approximately 7, over tens times greater than the factor of safety without the ties.

Table 4. Simulation comparisons between the CMU wall with and without continuous filament ties.

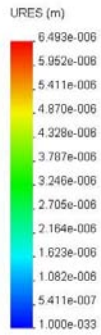
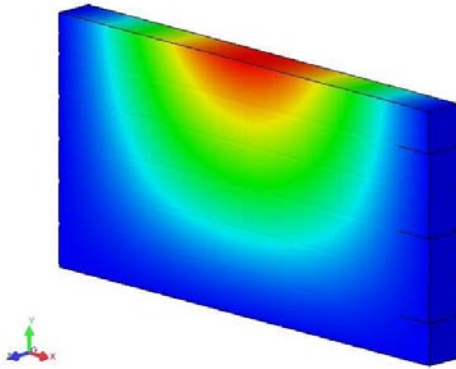
	CMU Wall without Continuous Filament Ties	CMU Wall with Continuous Filament Ties (polypropylene spacers)
100 mph wind (pressure = 0.2 psi)		
Max Stress:	$1.276 \times 10^5 \text{ N/m}^2$	$1.857 \times 10^5 \text{ N/m}^2$
Max Displacement:	$6.493 \times 10^{-6} \text{ m}$	$6.512 \times 10^{-6} \text{ m}$
FOS:	290	3300
Explosive Attack (pressure = 100 psi)		
Max Stress:	$6.38 \times 10^7 \text{ N/m}^2$	$8.652 \times 10^7 \text{ N/m}^2$
Max Displacement:	$3.25 \times 10^{-3} \text{ m}$	$3.26 \times 10^{-3} \text{ m}$
FOS:	0.58	6.7
Seismic Event (Peak Ground Acceleration = 1 “g” = 9.81 m/s²)		
Max Stress:	$6.89 \times 10^5 \text{ N/m}^2$	$7.54 \times 10^5 \text{ N/m}^2$
Max Displacement:	$8.16 \times 10^{-5} \text{ m}$	6.85×10^{-5}
FOS:	54	820

FOS = factor of safety (yield strength of material divided by maximum applied stress)

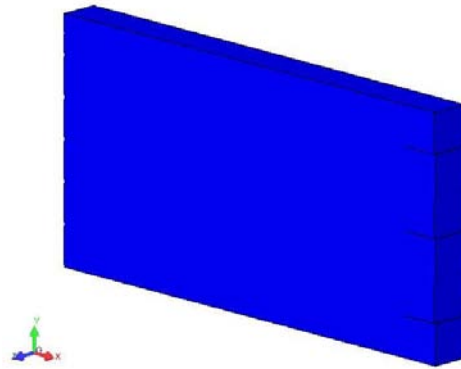
Figure 11 and Figure 12 show images from the 100-mph-wind and explosive-attack simulations of the walls with and without ties. The top of each figure shows the results for 100 mph winds (0.2 psi), and the bottom of each figure shows the results for an explosive blast (100 psi). The images on the left show the simulated displacement of the wall, and the images on the right show the simulated minimum factor of safety (if the factor of safety is greater than one, the color is blue (no failure); if the factor of safety is less than one, the color is red (denoting areas of failure)).

Figure 13 shows a section view of the region of maximum stress in the wall with ties during the explosive blast. Even though the simulated maximum stress is greater in the wall with ties than in the wall without ties, the stress is absorbed by the steel filaments within the mortar. The steel has a much greater yield strength than the concrete or the mortar (see Table 1). Therefore, the resulting minimum factor of safety for the wall with ties is still greater in the regions of maximum stress than without the ties.

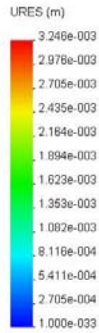
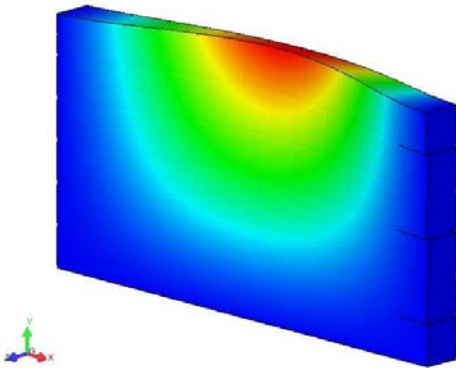
Model name: Short CMU Wall_no spacers
Study name: 100 mph Wind
Plot type: Static displacement-Plot1
Deformation Scale: 75



Model name: Short CMU Wall_no spacers
Study name: 100 mph Wind
Plot type: Design Check-Plot1
Criterion: Max von Mises Stress
Red < FOS = 1 < Blue



Model name: Short CMU Wall_no spacers
Study name: Explosive Attack
Plot type: Static displacement-Plot1
Deformation Scale: 75



Model name: Short CMU Wall_no spacers
Study name: Explosive Attack
Plot type: Design Check-Plot1
Criterion: Max von Mises Stress
Red < FOS = 1 < Blue

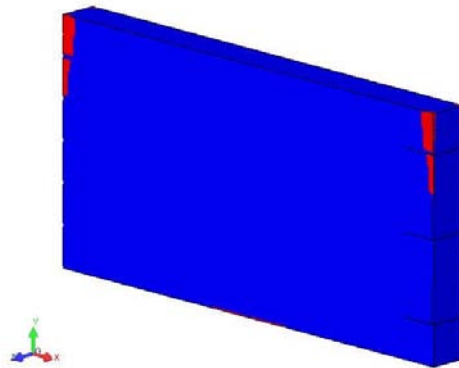


Figure 11. Results of lateral loading on a wall without ties for 100 mph wind (top) and explosive blast (bottom). Displacement plots are on the left, and factor of safety plots are on the right (the FOS plot shows only two colors: blue if FOS > 1 and red if FOS < 1).

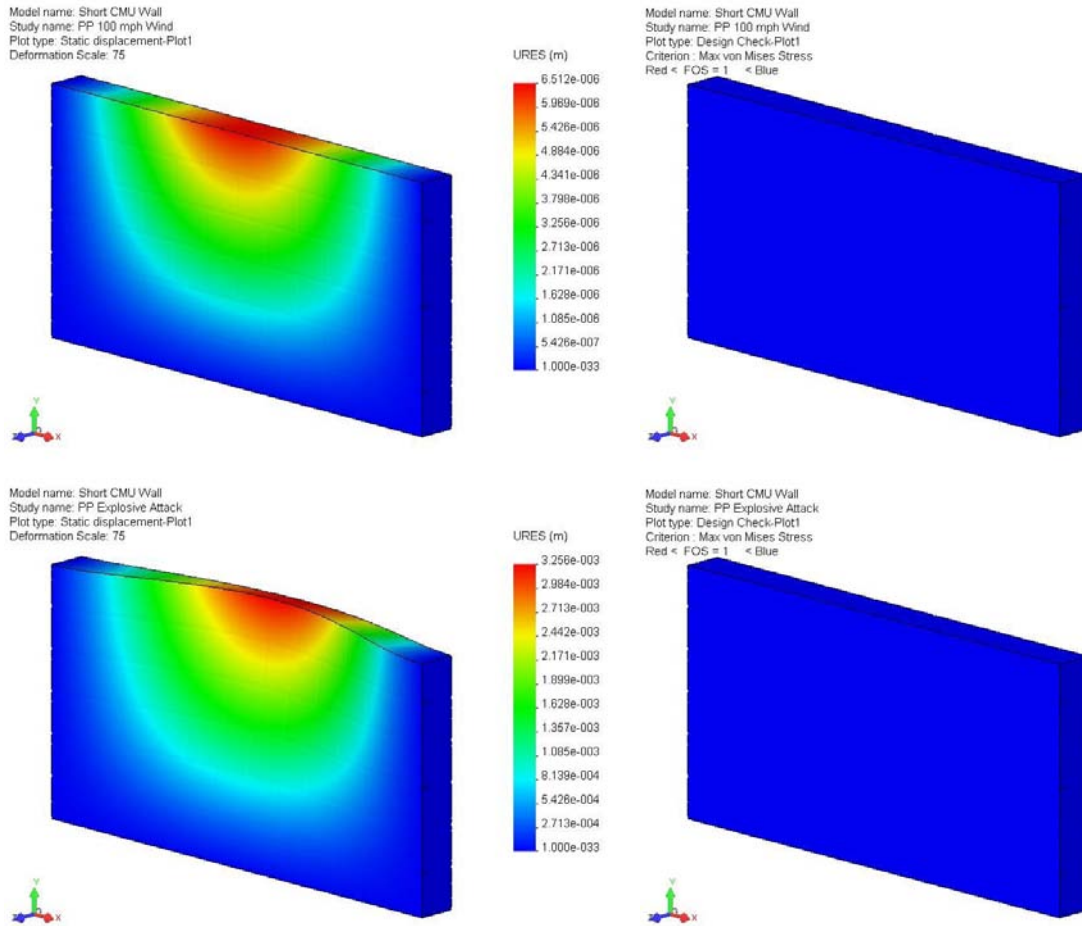


Figure 12. Results of lateral loading on a wall with ties (dual filaments with polypropylene short T-spacers) for 100 mph wind (top) and explosive blast (bottom). Displacement plots are on the left, and factor of safety plots are on the right (the FOS plot shows only two colors: blue if FOS > 1 and red if FOS < 1).

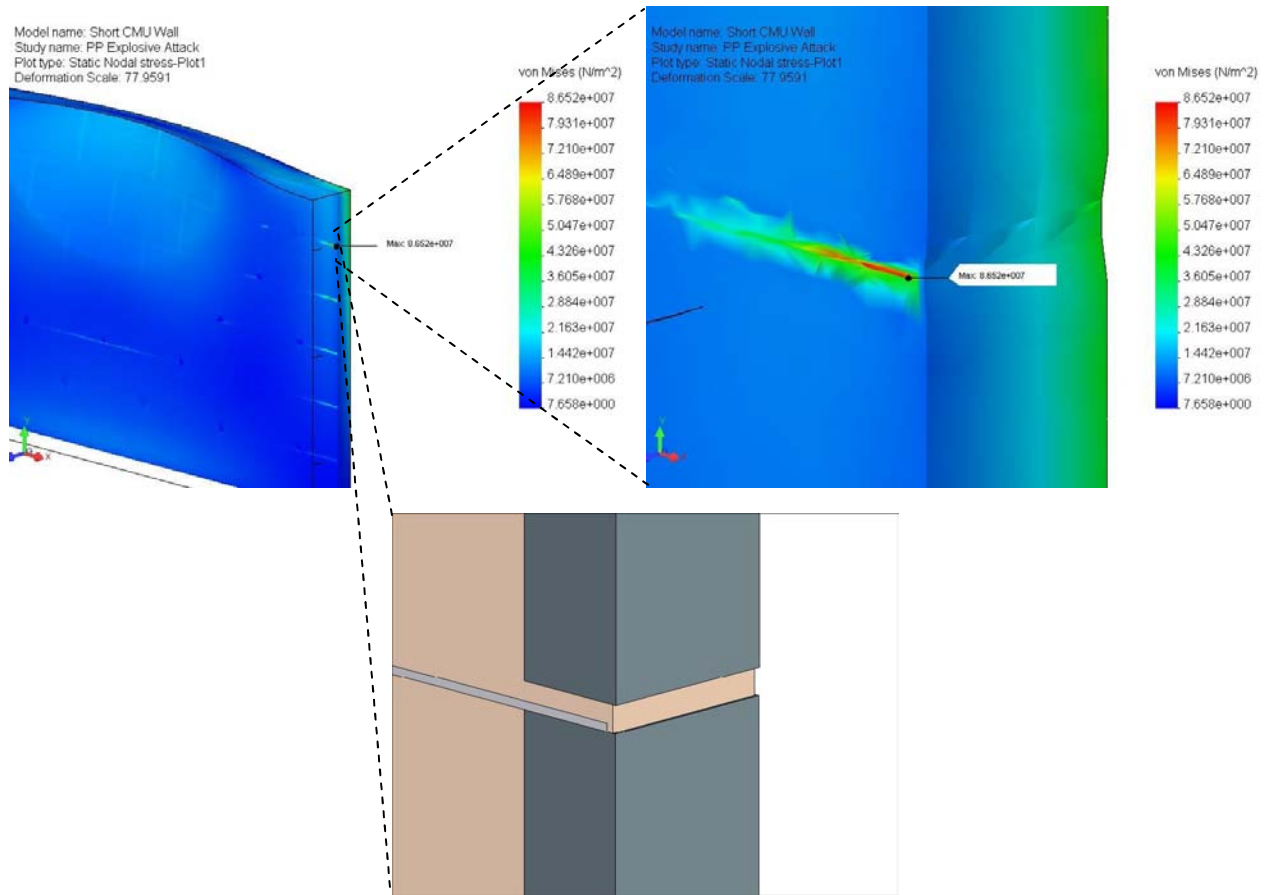


Figure 13. Top left: Maximum stress plot of the CMU wall with ties. Top right: Close-up image of the max stress on a section view of the CMU wall with ties. Bottom: Section view of the CMU wall that shows the steel filament in the mortar between the CMU blocks that absorbed the stress.

For the seismic scenario, Table 4 shows that simulations of the wall with and without the ties yield acceptable factors of safety. The simulation with the ties yields a factor of safety that is over ten times greater than the factor of safety without the ties. In addition, the maximum displacement of the simulated wall with ties is nearly 20% less than the maximum displacement without the ties. Figure 14 and Figure 15 shows the simulated displacement and stress distribution along the wall with and without the ties. In both cases, the simulated maximum stress occurs in compression at different locations along the wall. For the simulated wall without ties (Figure 14), the maximum stress is along the bottom of the wall, but for the simulated wall with ties (Figure 15), the maximum stress is above the first row of CMU blocks along the steel filament. Figure 16 shows a cutaway view of the simulated wall with ties, exposing the location of maximum stress along the steel filament.

It should be noted that the models of the static loading scenarios considered in this study may not accurately reflect the response of actual masonry walls subject to similar loading conditions. Constitutive relations governing the behavior of composite materials in contact with each other

(e.g., concrete, mortar, steel, polypropylene) were not rigorously defined or evaluated. Materials in contact with each other in the model were assumed to be fixed along the interface. In addition, behavior such as cracking and micro-fracturing and their impact on the overall integrity of the simulated wall were not considered. The purpose was to compare the impacts of various loading conditions on simulated CMU shear walls with and without the continuous filament ties. All other system parameters and boundary conditions were identical in each pair of simulations. Therefore, a preliminary assessment and comparison of the wall performance with and without the ties could be made. Physical experiments are still needed to verify the simulated results and observations made in this study.

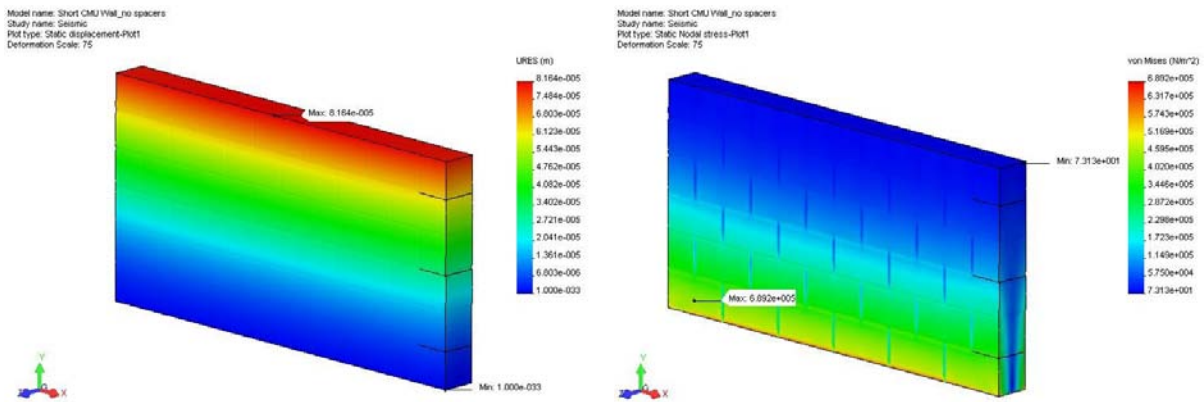


Figure 14. Simulated resultant displacement (left) and stress distribution (right) of CMU wall without ties for seismic event.

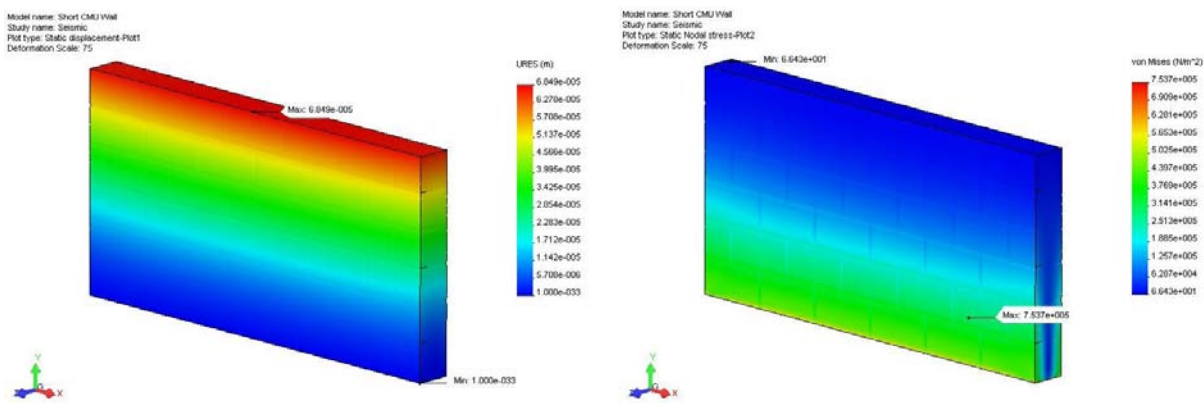


Figure 15. Simulated resultant displacement (left) and stress distribution (right) of CMU wall with ties for seismic event.

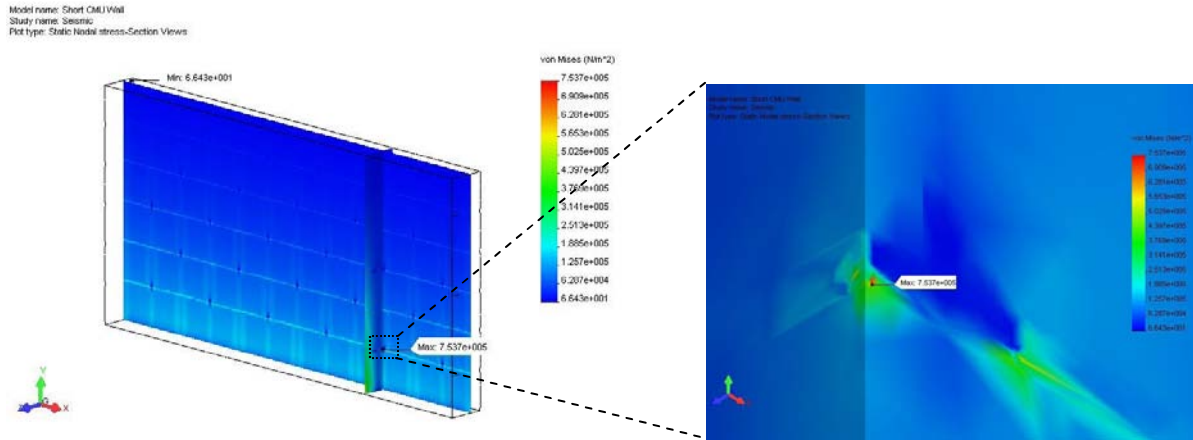


Figure 16. Cut-planes showing location of maximum simulated stress in the CMU wall with ties for the seismic scenario. In the expanded view on the right, the highest stresses are shown to occur along the steel filament under the polypropylene spacer (blue outline).

4. Summary

Finite-element analyses were performed to assess different materials and designs for proposed continuous filament ties and spacers developed by The Arquin Corporation. Based on the results of the static-loading simulations and cost comparisons, the following materials for the spacer designs are recommended: polypropylene, ABS, and polyethylene (high density). These materials performed well with regard to the simulated performance metrics of displacement and factor of safety, and they were the least expensive. These materials are also amenable to injection molding processes. With regard to the design, the small T-spacer design is recommended because of its acceptable performance, lowest cost, and increased functionality.

Simulations were also performed to evaluate the performance of a wall with and without ties subject to 100 mph winds, an explosive blast, and an earthquake. Results showed that while both simulated walls performed adequately when subject to 100 mph winds (0.2 psi) and lateral loads due to seismic ground motion (0.66 psi), only the wall with the ties (dual filaments with polypropylene short T-spacers) was able to withstand the explosive blast (100 psi). The steel filaments absorbed the maximum stresses and prevented the yield strength of the concrete and mortar from being exceeded. In addition, for the seismic scenario, the simulation of the wall with the ties yielded maximum displacements that were 20% less than those of the simulated wall without ties. In all scenarios evaluated, the simulated factor of safety with the ties was over 10 times greater than the factor of safety without the ties.

5. References

Callister, Jr., W.D., 2003, *Materials Science and Engineering, An Introduction*, 6th ed., John Wiley & Sons, New York.

International Building Code, 2003, International Code Council, Inc.

Petersen et al., 1996, Probabilistic Seismic Hazard Assessment for the State of California, United States Geological Survey (USGS) Open-File Report 96-706, U.S. Department of the Interior (online report available at: www.consrv.ca.gov/cgs/rghm/psha/ofr9608/).

Roberson, J.A., and C.T. Crowe, 1985, *Engineering Fluid Mechanics*, 3rd ed., Houghton Mifflin Co., Boston.

Trifunac, M.D. and A.G. Brady, 1975, On the correlation of seismic intensity with peaks of recorded strong ground motion, *Bull. Seismol. Soc. Amer.*, 65, 139-162.

Wald, D.J., V. Quitoriano, T.H. Heaton, and H. Kanamori, 1999, Relationships Between Peak Ground Acceleration, Peak Ground Velocity, and Modified Mercalli Intensity in California, *Earthquake Spectra*, 15(3), 557-564.

Distribution

Internal

1 MS-0701 P. Davies, 6100
1 MS-0701 J. Merson, 6110
1 MS-0735 R. Finley, 6115
1 MS-0735 C. Ho, 6115
1 MS-0201 J. Sinsabaugh, 10222
1 MS-0201 M. Johnston, 10222

2 MS-9018 Central Technical Files, 8944
2 MS-0899 Technical Library, 4536

External

Armando Quinones Sr.
The Arquin Corporation
P.O. Box 876
La Luz, NM 88337



Sandia National Laboratories